Modified genetic algorithms to model cluster structures in medium-sized silicon clusters: Si_{18}-Si_{60}

Ofelia Oña,[1] Victor E. Bazterra,[1,2] María C. Caputo,[1] Julio C. Facelli,[2] Patricio Fuentealba,[3] and Marta B. Ferraro[1,*]
[1]*Departamento de Física, Facultad de Ciencias Exactas y Naturales, Universidad de Buenos Aires, Ciudad Universitaria, Pab. I (1428), Buenos Aires, Argentina*
[2]*Center for High Performance Computing, University of Utah, 155 South 1452 East Rm 405, Salt Lake City, Utah 84112-0190, USA*
[3]*Departamento de Física, Facultad de Ciencias, Universidad de Chile, Casilla 653, Santiago 1, Chile*
(Received 17 October 2005; published 25 May 2006)

This paper presents the results obtained using a genetic algorithm (GA) to search for stable structures of medium-size silicon clusters. This is the third report in which a GA coupled with the MSINDO semiempirical molecular orbital program is used to find stable atomic cluster structures. The structures selected by the GA-MSINDO method were further optimized using the density functional theory (DFT). This combination of GA-MSINDO global optimization followed by DFT local optimization proves to be very effective for searching the structures of medium-size Si clusters. For most of the clusters studied here we report different structures with significant lower energy than those previously found using limited search approaches on common structural motifs. This demonstrates the need for global optimization schemes when searching for stable structures of medium-size silicon clusters.

DOI: 10.1103/PhysRevA.73.053203 PACS number(s): 36.40.−c

I. INTRODUCTION

The study of the structure and physical properties of atomic and molecular clusters is an extremely active area of research due to their importance, both in fundamental science and in applied technology, [2] such as the luminescence in nanostructured silicon clusters [3] and the appearance of silicon photonic crystals with applications in nanotechnology [4].

Existing experimental methods for structural determination seldom can obtain the structure of atomic clusters directly. Therefore, the calculation, using theoretical structures, and comparison with experimental values of their physical and optical properties is the most common way to obtain structural information of atomic clusters. The prediction of the structures of clusters with a small number of atoms is well understood. But in spite of their critical importance in understanding the transition from microscopic to macroscopic behavior of nanomaterials and their possible technological applications, the prediction of the structures and properties of medium-size (10–100 atoms) clusters is much less developed.

The investigations on Si_n clusters [5] have been directed by the formidable developments observed in the field of carbon clusters during the last two decades. Differences and similarities between both series of atomic clusters have been pointed out in numerous publications [6]. For instance, no fullerenelike structures have been identified for Si_n units, this is attributable to the sp^2 characteristic hybridization in fullerenes, which is more favorable for C_n than for Si_n units [7], i.e., silicon clusters of five atoms form three-dimensional compact structures while pure carbon clusters with ten or less atoms show linear and ring structures.

Clusters with up to ~10 atoms can be modeled using standard geometry optimization techniques in conjunction with quantum chemistry methods, such as the density functional theory (DFT), second order Møller Plesset, coupled clusters, etc. Systematic, global geometry optimizations of larger clusters is complex and time consuming due to the large number of possible structures [8] the time required for the calculation of their total energies, and the lack of effective methods to perform global searches. Nowadays, the global optimization of clusters with ~20 atoms is almost an intractable problem and inconsistent results on the structures of Si_n, $10 \leqslant n \leqslant 30$ clusters have been reported in the literature [5,6,9–15]. For these medium- to large-size clusters the option of using *ab initio* or DFT methods to calculate the cluster energies is limited due to the extremely large computer resources needed. For this reason the literature presents a great number of methods for searching structures of Si clusters using either very approximate energy approximations and/or minimization schemes based on local optimizations of plausible structural mottifs [16–19]. Jackson *et al.* [16] employed the big bang search algorithm, an unbiased and highly parallel method for searching cluster energy surfaces using the density-functional tight-binding (DFTB) method, and presented structures for silicon clusters with 20–27 atoms significantly more stable than any of those previously found. These structures neither resemble bulk silicon packing nor obey the rule of tricapped trigonal prisms stacking [8,17,18]. Yoo *et al.* [5] used a combined molecular mechanics-quantum mechanics procedure to search for Si_{21} and Si_{25} clusters finding some isomers with appreciably lower energy than those reported previously. They are also more spherical-like than the ones found by an unbiased search for the lowest-energy geometric structures of medium size-silicon clusters Si_n $(27 \leqslant n \leqslant 39)$ using a genetic algorithm combined with the tight-binding method [19]. These results appear to be in agreement with recent measurements

*Corresponding author. E-mail address: marta@df.uba.ar

of mobility of Si_n^+ silicon clusters showing that prolate and compact isomers can coexist for n between 25 and 33 [20,21]. Very recently Yoo and Zeng [22] used a computational approach that combines the unbiased basin-hopping (BH) global optimization method, employing two types of GGA (general gradient approximation) exchange correlation functionals BLYP and PBE [23] followed by an all-electron reoptimization using B3LYP/6-311G(2d) and PBE1PBE/6-311G(2d) to find new more stable structures for Si_{16}, Si_{17}, Si_{18}, and Si_{22}. In this work the authors kept a Si_6/Si_6 motif as the seed in their DFT-BH search. Similar techniques were used in the study of one of the largest studied silicon clusters, Si_{36},[6] introducing small modifications into several common structural motifs observed in nanostructures: cages, wires and fullerenes. But in subsequent work on Si_{36} we have shown [24] that a global search based in a GA-MSINDO approach followed by local optimization using DFT methodologies is able to find at least three structures of Si_{36} that have significant lower energy than those previously known in the literature [6]. This finding clearly highlights the importance of exploring the complete configuration space when searching for atomic clusters. Here, we report the use of the same approach to predict the structure of silicon clusters with 18–60 atoms.

In addition to the global structural searches discussed above, in this work we investigate the static dipole polarizabilities of the Si clusters generated here and explore the relationship between polarizability, bonding energy, and high occupied molecular orbital–low-unoccupied molecular orbital (HOMO-LUMO) gap with the cluster's size. The importance of using polarizability data to rationalize experimental observations has been highlighted [25], and therefore there is a considerable effort to obtain confidence on the reliability of the theoretical models used for its calculation. The dipole polarizability of silicon clusters with 9–120 atoms has been measured [1] and they can be used as guide posts in the search for stable structures of Si_n clusters. Jackson *et al.* [26] computed polarizabilities for compact and prolate structures of Si_n clusters ($n=20-28$, and $n=50$) and found that the charge density show a metallic-like response of the clusters to an external field. The calculated polarizabilities of these clusters are reproduced by jellium models of spheres and cylinders of similar dimensions. The experimental polarizabilities reported by Schäfer *et al.* [1] vary irregularly around the bulk limit ($\alpha_{bulk}=3.71$ Å^3/atom) for $n \geqslant 9$; i.e. 2.9, 5.5, 2.8, and 1.8 Å^3/atom for $n=9$, 10, 11, and 12, respectively. On the other hand, theoretical results reported in the literature are greater than 4.0 Å^3/atom [15,27,28]. Becker *et al.* [29] have also reported experimental evidence that Si_n clusters with $60 \leqslant n \leqslant 120$ are characterized by mean polarizabilities below the bulk limit. There are also theoretical results for silicon clusters up to 13 atoms [15,27,28,30–32], most of them employing the DFT methodology.

It is also known that the HOMO-LUMO gap correlates well with the polarizability of an atomic cluster, being easier to polarize those systems with a smaller HOMO-LUMO gap [33]. Pouchan *et al.* [30] found a correlation between polarizability of Si_n ($n=3-10$) and the size of the energy gap between symmetry-compatible bonding and antibonding molecular orbitals, that is the "allowed gap," instead the HOMO-LUMO gap. However, this correlation has not been verified for medium-size clusters.

Here we present stable structures and polarizabilities for Si_{18}, Si_{20}, Si_{21}, Si_{22}, Si_{24}, Si_{26}, Si_{30}, Si_{32}, and Si_{34}, to demonstrate the validity of the method in silicon clusters with structures that are well characterized using DFT methods [10,34–36] and present different structures for larger clusters that have not been previously studied in detail, Si_{40}, Si_{46}, and Si_{60}. We have included Si_{60} in our studies due to its possible similarity with the analog C_{60}.

II. METHODOLOGY

In any GA implementation it is necessary to define a genome with enough information to calculate the associated fitness function. For the case of atomic clusters, the genome is quite simple because there are no symmetry or periodicity relationships that constrain the parameters in the genome. The genome is given as an array containing the coordinates of the atoms. This array has dimension $3N$, were N is the number of atoms in the cluster. Moreover, any genetic operator, mating, crossover, mutation, etc., applied to this genome produces a valid individual, i.e., a possible structure for the desired cluster size.

The first population, of size N_{pop}, is constructed by generating a set of atomic coordinates using random numbers. These random numbers, used to define the atomic positions in the cluster, belong to specific intervals selected according to the expected dimensions of the cluster; these restrictions have been included to avoid sampling in nonphysical configurations. The distances between any pair of atoms are calculated and compared with a set of rules that guarantees that they are within the normal values for silicon interatomic distances, otherwise the structure is rejected. This set of rules is designated to eliminate from the initial population all those structures that are evidently unphysical. There are basically two rules, the first states that if any pair of atoms is closer than a minimal distance (r_1) the structure will be rejected, the second rule states that if any atom is at a distance larger than r_2 to any other atom in the cluster the structure also will be rejected.

The GA operations of mating, mutation, and selection are used to evolve one generation into the next. In addition, for the larger clusters we have augmented these operations on the genome by using our implementation [37] of the real space "cut and split" operator introduced by Johnson and Roberts [38]. The population replacement is done through the steady-state genetic algorithm, which typically replaces only a portion of the individuals in each generation [39–41]. This technique is also known as elitism, because the best individuals among the population, 50% in our case, are copied directly into the next generation. The criteria for fitness probability, selection of the individuals, and mutation are discussed in detail in Ref. [42]. Like any stochastic minimization procedure the GA should be run several times to guarantee that the resulting structures are independent of the initial population and statistically significant.

The MGAC package has been implemented in C^{++} language using parallel techniques (MPI), making it very por-

table as well as easy to maintain and upgrade. Our parallel MGAC implementation of the parallel GA (PGA) is particularly efficient [43].

Using the information contained in the genomes the energy of each individual was evaluated and its structure relaxed to its local minimum. The methodology used here does not take into account any symmetry constraint. All the energy calculations for the GA optimizations were done using the MSINDO code. The optimizations used approximately 20–30 individuals for clusters with less than 40 silicon atoms, while the number of individuals was increased for larger clusters reaching 40 individuals for Si_{60}. The number of individuals was taken approximately as 50% of the number of free parameters in the optimization in Ref. [24], but we have verified that the smaller populations chosen here are large enough to have the required diversity to assure a good description of the configuration space. For the smaller clusters the GA converged in ~30 generations, while for Si_{46} and Si_{60} the GA optimization required more than 200 generations to converge.

The GA procedure was repeated several times employing different initial populations to confirm that the final selection of isomers was independent from the initial population. Populations were considered converged when the standard deviation of the energies in the population reaches 0.1 eV, for Si_{18} to Si_{24}, and from 0.2 eV, for Si_{25}, to 0.4 eV for Si_{60}. The structures in the final population were manually classified selecting a set of structures with a significant diversity for further refinement. All the structures in the population with significantly different features were considered for further analysis. The geometry of these isomers was locally optimized using density functional methods with the B3PW91 exchange correlation functional using the LanL2DZ basis set and Los Alamos pseudopotential [44] to reduce the computational cost associated with the larger cluster. Additional calculations using the Stuttgart pseudopotential with its corresponding basis set, SDDALL [45], and the B3PW91 exchange correlation functional were performed to verify the sensitivity of the results with the selection of the pseudopotential. Vibrational frequencies were calculated for the optimized structures to check that no imaginary frequencies are present, confirming that the isomers presented here correspond to true minima of the potential energy.

In this paper we also have evaluated the static dipole polarizabilities for each final B3PW91-LanL2DZ and B3PW91-SDDALL stable structures of Si_n. All the DFT calculations have been done using the Gaussian package of programs [46].

III. RESULTS AND DISCUSSION

Figure 1 displays the stable structures obtained for the clusters Si_{18}-Si_{40}, Si_{46}, and Si_{60} employing the B3PW91-SDDALL scheme for their final local minimization and their corresponding binding energy per atom. The corresponding structures employing the B3PW91-LanL2DZ basis set are very similar to those of Fig. 1, most of them exhibit little differences in bond lengths and bond angles. Those structures for which the relaxed B3PW91-LanL2DZ isomers are not quite similar to the B3PW91- SDDALL ones are available free of charge [47]. The isomers enclosed into frames are very similar to those that have been previously reported in the literature [6,19,26,48,49]. In the Fig. 1, for the most stable isomer of each cluster, we have drawn the quantities L_x, L_y, and L_z, (measured in Å) representing the maximum extension of each isomer along the directions of its principal axis of inertia. The axes are labeled such that the modules of L_i are in rank order, i.e. $L_x \geq L_y \geq L_z$. The values of the L_i (L_x, L_y, and L_z) for all the isomers studied here are also included in the Supplementary Material session [47]. It is apparent from these data and from Fig. 1 that most of the isomers are prolate, but some of them are compact: Si_{24}-d, Si_{34}-b and Si_{46}-a.

In Table I we present the binding energies per atom, dipole polarizabilities per atom, energy gap, and dipole moment of all the clusters studied here. The binding energies are based on calculated silicon atomic energies of −101.536, and −101.429 eV, for the B3PW91-SDDALL and B3PW91-LanL2DZ methods respectively. In addition we have included the calculated binding energies per atom and the dipole moments of other structures reported in the literature by other authors [5,16,22,49], that kindly provided us the geometries of their ground states. The calculations of the properties of these structures were performed using the B3PW91-SDDALL and B3PW91-LanL2DZ approaches without further local optimizations. For most clusters, our approach is able to find numerous stable structures with higher binding energies, i.e., more stable, than the lowest one obtained by previous approaches based on lattice replacements and the local optimization of known structural motifs [5,16,22,49]. This becomes even more apparent as the size of the clusters grow. The locally refined structures are slightly more stable than the MGAC-MSINDO structures, but even the MGAC-MSINDO structures are more stable than the previously determined structures of Si_{18}, Si_{20}, Si_{21}, Si_{22}, Si_{24}, Si_{26}, Si_{40}, and Si_{60}. This finding highlights the importance of exploring the complete configuration space when searching for atomic cluster structures. Some of the structures provided by other authors exhibit imaginary frequencies indicating that for the methods used here they do not correspond to an actual local minima of the energy, this fact is indicated in the table with an [a]. Some compact isomers of Si_{30}, Si_{32}, and Si_{34} taken from the same sources [18], are more stable than ours. An inspection of these structures and the one given in Ref. [50] for Si_{40}, shows that these are endohedral of structures, i.e., they correspond to $Si_2@Si_{28}$, $Si_4@Si_{28}$, $Si_4@Si_{30}$, and $Si_6@Si_{34}$, which exhibit several hypervalent silicon atoms. While it is well known that hypervalent states are possible for silicon [18,50], the MSINDO energies of these structures are 4.35, 5.71, 5.44, and 9.25 eV, respectively, higher than those for the corresponding best MGAC/MSINDO isomers. This is an indication that the MSINDO is not able to reproduce the correct energy ranking of structures with silicon hypervalent atoms, leading to the rapid elimination of these structures in the population of the GA.

Figure 2 depicts the calculated binding energies per atom (BE/atom) with both the B3PW91-LanL2DZ and B3PW91-SDDALL approaches for the most stable clusters found in this work, as a function of the cluster size. The values in-

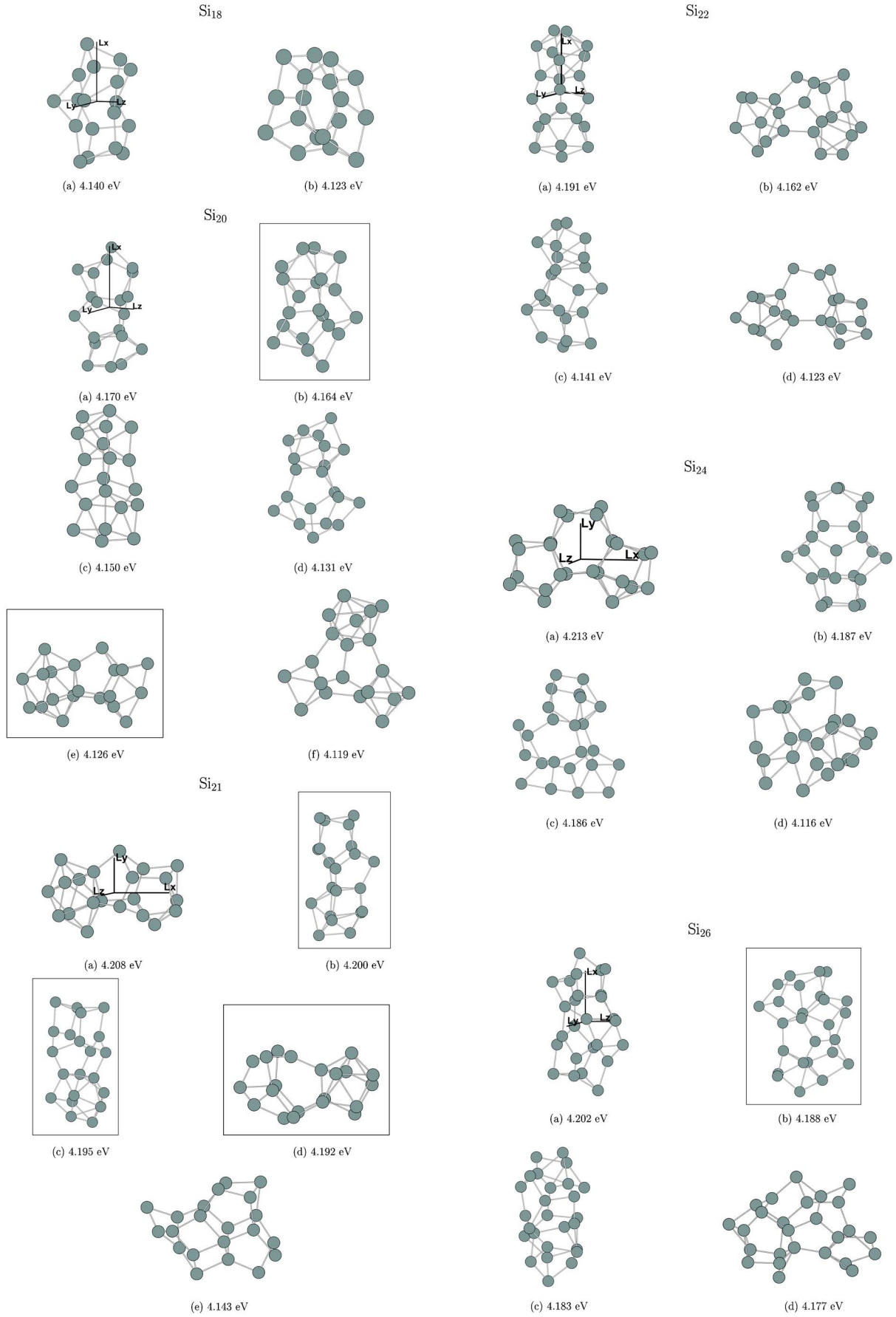

FIG. 1. (Color online) Optimized structures for stable Si_n $n=18,20,21,22,24,26,30,32,34,40,46,$ and 60) clusters, at the B3LYP-SDDALL level of theory. The structures similar to those reported in the literature are enclosed into frames.

Si_{26} (*Continued*)

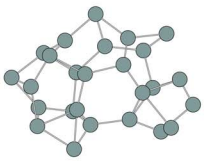

(e) 4.175 eV

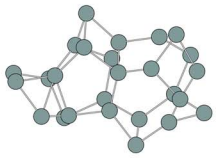

(f) 4.174 eV

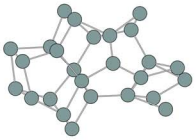

(g) 4.172 eV

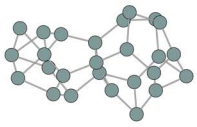

(h) 4.156 eV

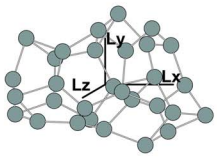

(a) 4.247 eV

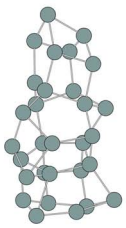

(b) 4.226 eV

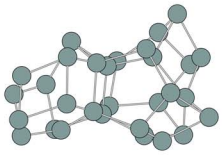

(c) 4.224 eV

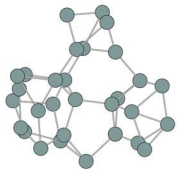

(d) 4.210 eV

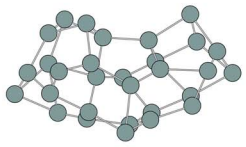

(e) 4.149 eV

Si_{32}

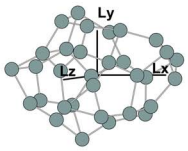

(a) 4.279 eV

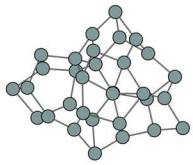

(b) 4.269 eV

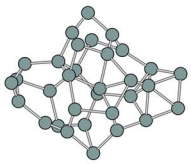

(c) 4.256 eV

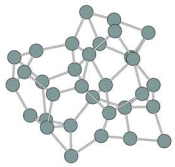

(d) 4.255 eV

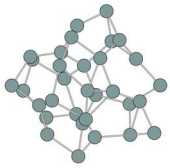

(e) 4.250 eV

Si_{34}

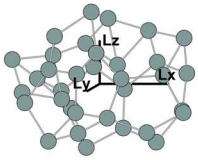

(a) 4.255 eV

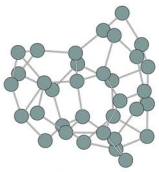

(b) 4.243 eV

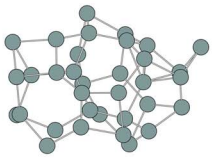

(c) 4.236 eV

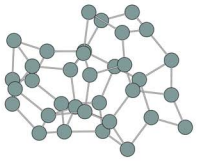

(d) 4.228 eV

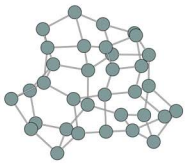

(e) 4.216 eV

Si_{40}

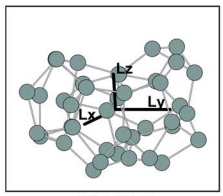

(a) 4.290 eV

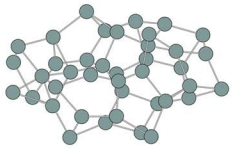

(b) 4.280 eV

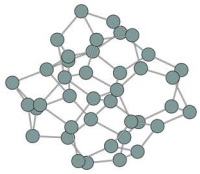

(c) 4.260 eV

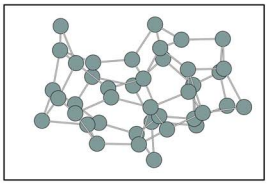

(d) 4.248 eV

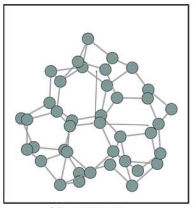

(e) 4.240 eV

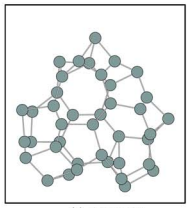

(f) 4.227 eV

Si_{46}

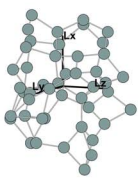

(a) 4.243 eV

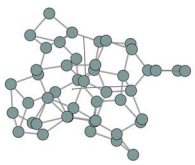

(b) 4.242 eV

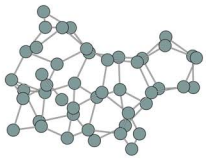

(c) 4.223 eV

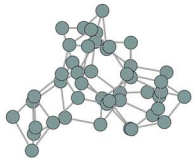

(d) 4.219 eV

FIG. 1. (Continued).

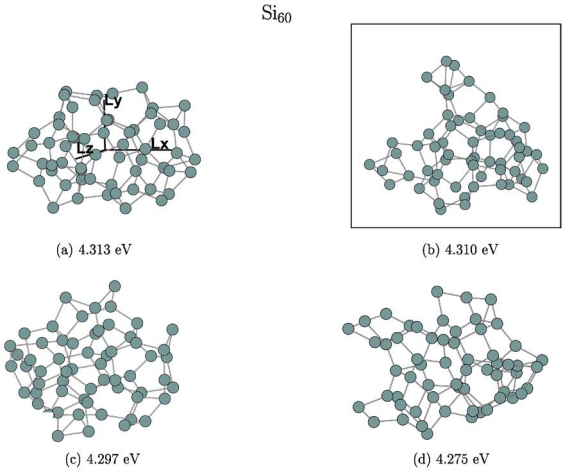

FIG. 1. (Continued).

crease slightly when the number of atoms increases, but this increase is not monotonic. The behavior is similar for both methodologies and reproduces the features observed by other authors in the smallest clusters of the series, to our knowledge. Our calculated binding energies for the most stable clusters, ranging from 4.140 to 4.313 eV (SDDALL) and from 4.356 to 4.592 eV (LANL2DZ) are slightly higher than the average experimental value of ~3.6 to 4.0 eV, reported by Bachels and Schäfer [50] for clusters of these sizes.

Using a simulated annealing combined with a tight-binding molecular dymamics methodology, proptotypes of stuffed fullerenelike cages were studied for Si_{40} [51]. None of the six most stable isomers found in this work resemble a cage structure. However, calculations using both, B3PW91-SDDALL and B3PW91-LanL2DZ, for the structure informed in Ref. [51], show that this structure is also a good candidate for the most stable isomer, and according to our calculations it presents one imaginary frequency, and a binding energy of 4.286 eV/atom. As discussed above, most likely this structure is rapidly eliminated from the GA population due to the overestimation by the MSINDO of the energies of structures with hypervalent silicon atoms. The binding energy per atom of our optimized structures is 4.29 eV/atom which is slightly larger than the experimental estimations of about 3.95 eV/atom [50,52].

We report also the results corresponding to the four best isomers of Si_{60} produced by our approach. We include in Table I the binding energies, polarizabilities, HOMO-LUMO gap, and dipole moments corresponding to the geometries of the stuffed structures SF1 and SF2 reported in Ref. [49]. Our Si_{60}-a is very similar to the SF1 structure. Isomer Si_{60}-d relaxes to Si_{60}-b for the LanL2DZ basis set. All our isomers, at the level of calculation presented here, are more stable than the ground state of Sun *et al.* [49], which according to our calculations presents five imaginary frequencies.

Figure 3 displays the behavior of the HOMO-LUMO gap for the most stable isomers for both basis sets. The gap is between 0.77 and 2.25 eV, approximately. The gap rapidly decreases with the number of atoms in the cluster until $n=30$, then it is almost constant approaching the bulk gap of around 0.65 eV obtained at a similar level of calculation [53]. In general, the gap shows little sensitivity to the method used in the calculation.

The polarizabilities evaluated using the B3PW91-SDDALL are in the range $\approx 4.87-5.78$ Å^3/atom, while those calculated with the B3PW91-LanL2DZ, are in the range $\approx 4.61-5.42$ Å^3/atom, and there is no difference on their tendence with respect to the cluster size, as it is depicted in Fig. 4. The calculated values are in the same range of those calculated by other authors. For instance, Jackson *et al.* [54] reported local density approximation polarizabilities for Si_{20} and Si_{21} of 4.83 and 4.58 Å^3/atom. In Fig. 4 the vertical bars on the SDDALL and LanL2DZ result represents the polarizability's dispersion of values among all the clusters studied here for each number of atoms. For the experimental data plotted in this figure the experimental error bars [1] are also included. It is apparent that the experimental values are always smaller than the calculated ones. Unfortunately, the comparison between experimental and calculated polarizabilities is difficult because the experimental procedure [1] does not determine their absolute values; it is always measured relative to the polarizability of ^{13}Al which has been extracted from a theoretical prediction [55]. In order to investigate the possibility that the discrepancy observed between the experimental and calculated data arises from an incorrect value of the polarizability used as a reference, we have performed a least-squared regression between the theoretical and experimental predictions.

The χ^2 confidence estimator for the correlation is defined as

$$\chi^2 = \sum_{i=1}^{12} \left(\frac{a y_i - t_i}{\sigma_i} \right)^2, \tag{1}$$

where the sum runs over the 12 cluster sizes for which there are experimental data among our theoretical predictions. y_i, σ_i, and t_i, are the experimental values, their errors, and the theoretical calculations, respectively. The value of the χ^2 at the minimum, obtained for $a=1.53$, yields $\chi^2=9.2$ for 11 degrees of freedom, which corresponds to a χ^2 probability of 61%. This indicates a good level of agreement between the theoretical predictions and the rescaled experimental data.

TABLE I. B3PW91–SDDALL and B3PW91–LanL2DZ binding energies per atom (in eV/atom), dipole polarizability per atom (Å^3/atom), HOMO-LUMO gap (in eV), and dipole moment (in debye) for the Si_n.

	SDDALL				LANL2DZ			
Isomers	BE (eV/atom)	(α/atom)	gap (eV)	μ (debye)	BE (eV/atom)	(α/atom)	gap (eV)	μ (debye)
Si_{18}-a	4.140	5.04	1.721	0.745	4.369	4.69	1.549	0.685
Si_{18}-b	4.123	5.06	1.360	0.945	4.319	4.76	1.173	1.318
Si_{18}[b]	4.110[a]			1.068	4.336[a]			1.181
Si_{20}-b	4.170	5.17	1.744	1.568	4.370	4.98	1.450	1.194
Si_{20}-b	4.164	4.87	1.752	1.437	4.404	4.63	1.481	1.898
Si_{20}-c	4.150	5.29	1.469	1.968	4.337	4.92	2.289	1.955
Si_{20}-d	4.131	4.93	1.513	3.148	4.336	4.75	1.428	3.312
Si_{20}-e	4.126	5.07	2.056	1.547	4.289	4.79	1.869	2.464
Si_{20}-f	4.119	5.37	1.409	4.266	4.311	5.22	1.235	0.700
Si_{20}[c]	3.995			1.390	4.270			1.330
Si_{20}[d]	4.012			1.781	4.243[a]			1.796
Si_{21}-a	4.208	5.00	2.207	1.451	4.391	4.71	1.867	2.783
Si_{21}-b	4.200	5.06	1.979	0.810	4.385	4.75	1.724	1.36
Si_{21}-c	4.195	5.12	1.848	0.968	4.385	4.79	1.698	1.426
Si_{21}-d	4.192	5.03	2.291	0.444	4.381	4.69	1.958	1.604
Si_{21}-e	4.143	5.26	1.443	1.668	4.377	4.84	1.553	1.965
Si_{21}[c]	3.950			0.010	4.186[a]			0.123
Si_{21}[d]	4.047			1.593	4.305[a]			1.719
Si_{22}-a	4.191	5.20	1.727	2.251	4.356	4.87	1.845	2.886
Si_{22}-b	4.162	5.09	1.873	2.264	4.376	4.78	1.916	3.403
Si_{22}-c	4.141	5.18	1.760	0.180	4.339	4.80	1.964	1.642
Si_{22}-d	4.123	5.26	1.750	2.336	4.298	4.98	1.479	3.558
Si_{22}[b]	4.170[a]			2.099	4.390[a]			2.291
Si_{22}[c]	4.085			0.126	4.015			0.103
Si_{22}[d]	4.012			3.547	4.044			3.533
Si_{24}-a	4.213	5.18	1.760	0.960	4.412	4.90	1.777	1.856
Si_{24}-b	4.187	5.24	1.761	1.977	4.430	4.85	1.571	1.354
Si_{24}-c	4.186	5.16	2.088	2.174	4.381	4.84	1.404	3.108
Si_{24}-d	4.116	5.20	1.720	2.040	4.412	4.92	1.309	4.119
Si_{24}[c]	4.015			2.043	4.271			2.250
Si_{24}[d]	4.044[a]			2.324	4.269[a]			2.568
Si_{26}-a	4.202	5.15	1.391	1.524	4.440	4.86	1.195	1.052
Si_{26}-b	4.188	5.28	1.231	1.898	4.435	5.03	1.349	2.664
Si_{26}-c	4.183	5.15	1.408	0.574	4.403	4.81	1.530	0.958
Si_{26}-d	4.177	5.15	1.656	4.553	4.390	4.79	1.306	4.189
Si_{26}-e	4.175	5.25	1.461	2.947	4.410	4.88	1.130	2.424
Si_{26}-f	4.174	5.31	1.610	1.989	4.400	5.07	1.299	2.346
Si_{26}-g	4.172	5.36	1.290	1.988	4.417	5.00	1.253	2.853
Si_{26}-h	4.156	5.57	1.178	1.962	4.383	5.22	1.123	4.578
Si_{26}[c]	4.090[a]			2.382	4.378[a]			2.965
Si_{26}[d]	4.037[a]			3.763	4.255			4.258
Si_{30}-a	4.247	5.22	1.037	3.396	4.483	4.97	1.021	3.414
Si_{30}-b	4.226	5.26	1.418	3.679	4.483	5.05	1.289	1.800
Si_{30}-c	4.224	5.29	1.421	3.684	4.472	5.06	1.144	2.317
Si_{30}-d	4.210	5.43	1.044	2.464	4.456	5.14	0.829	2.953
Si_{30}-e	4.149	5.32	0.874	5.894	4.422	5.14	1.360	4.770
Si_{30}[b]	4.258[a]			0.566	4.551			0.59

TABLE I. (*Continued.*)

	SDDALL				LANL2DZ			
Isomers	BE (eV/atom)	(α/atom)	gap (eV)	μ (debye)	BE (eV/atom)	(α/atom)	gap (eV)	μ (debye)
Si_{32}-a	4.279	5.04	0.966	3.044	4.532	4.70	0.898	3.500
Si_{32}-b	4.269	5.16	1.267	5.337	4.515	4.83	1.180	4.986
Si_{32}-c	4.256	5.20	1.241	2.400	4.499	4.90	1.029	2.098
Si_{32}-d	4.255	5.09	1.277	2.818	4.498	4.83	1.001	5.087
Si_{32}-f	4.250	5.09	1.125	4.520	4.491	4.79	1.106	4.047
Si_{32}[b]	4.279			0.938	4.456			0.969
Si_{32}-a[b]	4.266			0.687	4.555			0.584
Si_{34}-a	4.255	5.08	1.112	5.302	4.471	4.73	0.964	5.302
Si_{34}-b	4.243	5.07	1.208	1.477	4.515	4.74	0.970	1.478
Si_{34}-c	4.236	5.18	1.048	6.358	4.483	4.95	0.777	6.359
Si_{34}-d	4.228	5.15	1.176	5.030	4.502	4.63	1.329	5.031
Si_{34}-e	4.216	5.37	1.124	4.501	4.443	5.00	1.119	4.502
Si_{34}[b]	4.283			2.506	4.571			2.768
Si_{40}-a	4.290	5.08	1.088	3.180	4.563	4.68	1.087	2.793
Si_{40}-b	4.280	5.29	1.106	1.819	4.533	5.12	0.917	1.109
Si_{40}-c	4.260	5.29	0.977	2.468	4.545	4.83	0.974	4.357
Si_{40}-d	4.248	5.30	0.995	2.032	4.515	5.07	0.919	2.866
Si_{40}-e	4.240	5.28	1.036	3.272	4.494	4.87	1.102	4.293
Si_{40}-f	4.227	5.28	0.985	2.021	4.494	4.87	1.082	4.424
Si_{40}[e]	4.286[a]			1.157	4.572[a]			1.241
Si_{46}-a	4.243	5.43	1.040	4.272	4.517	5.16	0.896	3.267
Si_{46}-b	4.242	5.58	1.022	3.448	4.486	5.29	1.151	4.712
Si_{46}-c	4.223	5.75	0.854	8.402	4.475	5.39	0.956	4.726
Si_{46}-d	4.219	5.78	0.915	5.964	4.461	5.42	0.862	6.986
Si_{60}-a	4.313	5.26	0.851	2.508	4.592	4.95	0.846	2.567
Si_{60}-b	4.310	5.55	1.091	4.407	4.571	5.19	0.784	4.554
Si_{60}-c	4.297	5.32	1.203	3.444	4.557	5.12	0.885	3.893
Si_{60}-d	4.275	5.45	1.194	7.179	4.571	5.19	0.783	4.574
Si_{60}-SF1[f]	4.239[a]			3.196	4.520[a]			3.196
Si_{60}-SF2[f]	4.232[a]			1.869	4.504[a]			1.989

[a]Imaginary frequencies.
[b]Reference [19].
[c]Compact isomers from Refs. [5,26].
[d]Prolated isomers from Ref. [26].
[e]From Ref. [51].
[f]From. Ref. [49].

The same type of regression has been found for the polarizabilities taken from theoretical predictions of other authors [26]. It is worth noting that recently exhaustive theoretical calculations of the dipole polarizability of an aluminum atom [56] present a deviation of approximately 26% with respect to the value used in the atomic cluster measurement [1]. The use of the new theoretical value should increase the experimental dipole polarizabilities of silicon clusters giving a $\chi^2 = 24.5$, corresponding to a marginal concordance of 1% to be compared to the complete disagreement probability of 10^{-8}% obtained when using the experimental published results.

The SDDALL calculated polarizabilities (Å^3/atom) together with the inverse of the gap (eV^{-1}) are plotted out in Fig. 5 as a function of the number of Si atoms in the cluster. The selection of the inverse of the gap to make the regression is inspired in the fact that according to the simple perturbation theory, using the one electron wave function, the gap between the occupied and unoccupied molecular orbitals controls the magnitude of α. The linear fit for the α values versus the inverse of the gap between the highest occupied and the lowest unoccupied molecular orbitals: E_g^{-1} gives the relation

$$\alpha = 0.58E_g^{-1} + 4.96.$$

For Si_n ($n=3-10$) Pouchan *et al.* [30] found the correlation

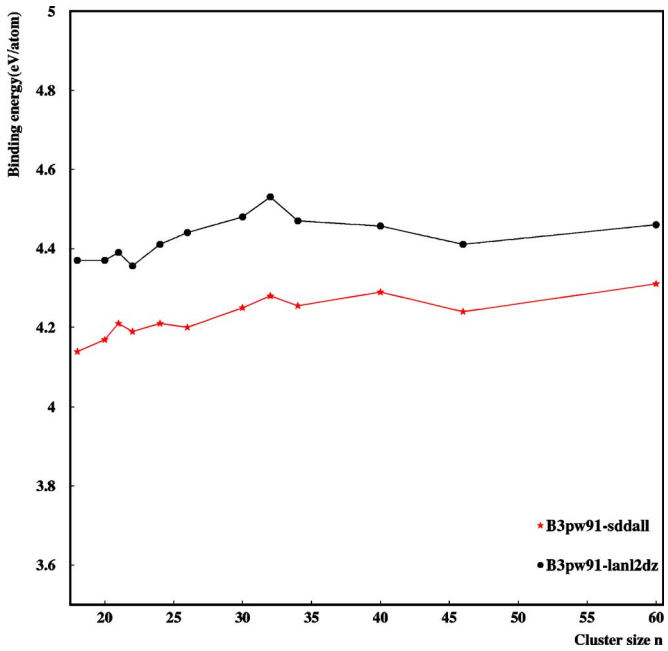

FIG. 2. (Color online) Binding energies in eV/atom as a function of the cluster size calculated within B3PW91-SDDALL and B3PW91-LanL2DZ methods.

$$\alpha = 0.51E_{ga}^{-1} + 4.48.$$

between the polarizability and the size of the energy gap between symmetry-compatible bonding and antibonding molecular orbitals, which they call "gap allowed" (E_{ga}). The use of a different definition of the gap explains the difference in the slope.

IV. CONCLUSIONS

A new strategy to find stable isomers of silicon clusters has been presented. The principal advantage of the hybrid technique proposed here is that it does not need to make any assumptions on the symmetry or type of the cluster structures, allowing for a full exploration of the complete configuration space available for the cluster geometry. Moreover the use of GA for the exploration of the space allows for an efficient search into those regions of the configuration space that represent the desirable low-energy configurations. This global search was possible due to the use of a semiempirical energy function because computational limitations still make these searches difficult when using *ab initio* methods for medium-size clusters.

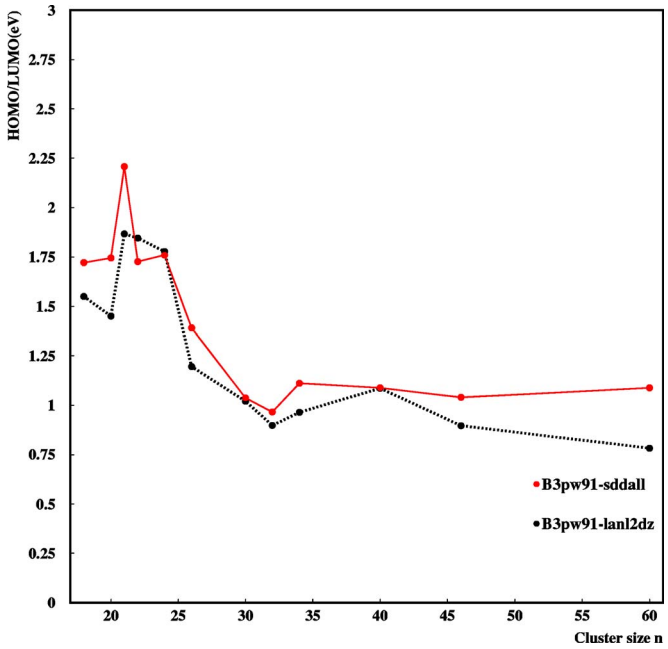

FIG. 3. (Color online) HOMO-LUMO gap in eV as a function of the cluster size calculated within B3PW91-SDDALL and B3PW91-LanL2DZ methods.

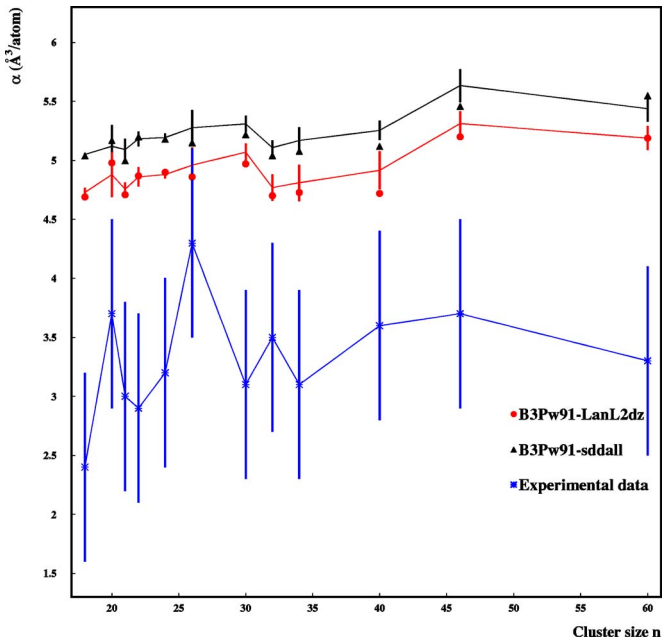

FIG. 4. (Color online) Comparison between B3PW91 atomic dipole polarizability and experimental data: (▲) SDDALL basis set; (•) LanL2DZ basis set; (*) experimental data from Ref. [1].

With the exception of Si_{30}, Si_{32}, and Si_{34}, where the MSINDO fails to reproduce the correct ranking of endohedral structures, it is clearly demonstrated that previous approaches, using local optimization of plausible structural motifs, may produce structures that are significantly higher in energy than those presented here. This justifies the need for global optimization schemes when searching for stable structures of medium-size silicon clusters.

ACKNOWLEDGEMENTS

Financial support for this research by the University of Buenos Aires (UBACYT-X035) and the Argentinean CONICET (PIP-5119/05) is gratefully acknowledged. JCF acknowledges the support from the International and Chemistry Divisions of NSF through Grant No. INT-0071032. P.F. acknowledges the support by FONDECYT under Grant No. 1050294 and the Millennium Nucleus for Applied Quantum Mechanics and Computational Chemistry. The authors thank Profressor K. Jackson for providing the structures of Si_{20}-Si_{28} and Dr. Q. Sun and Profressor Y. Kawazoe for providing the geometries of their stuffed fullerene structures SF1 and SF2 of Si_{60} clusters. The software for this work used the GAlib genetic algorithm package, written by Matthew Wall at the Massachusetts Institute of Technology. The Cen-

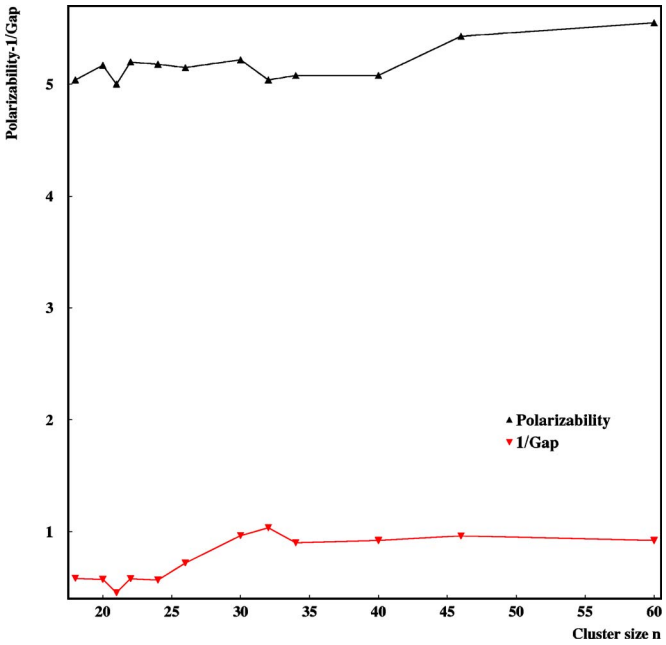

FIG. 5. (Color online) Polarizability of Si_n (▲) as a function of the cluster size, *n*, together with the inverse of the HOMO-LUMO gap (▼).

ter for High Performance Computing provided computer resources in the Arches cluster for this project. The Arches cluster was partially funded by NIH-National Center for Research Resource (Grant No. 1S10RR017214-01).

[1] R. Schäfer, Schletcht, J. Woenckhaus, and J. A. Becker, Phys. Rev. Lett. **76**, 471 (1996).
[2] U. Landman, R. N. Barnett, A. G. Scherbakov, and P. Avouris, Phys. Rev. Lett. **85**, 1958 (2000).
[3] K. D. Hirschman *et al.*, Nature (London) **384**, 338 (1996).
[4] S. Y. Lin *et al.*, Nature (London) **394**, 251 (1998).
[5] S. Yoo *et al.*, J. Am. Chem. Soc. **125**, 13318 (2003).
[6] Q. Sun, Q. Wang, S. Waterman, P. Jena, and Y. Kawazoe, Phys. Rev. A **67**, 063201 (2003).
[7] M. Menon and K. R. Subbaswamy, Chem. Phys. Lett. **219**, 219 (1994).
[8] K. M. Ho *et al.*, Nature (London) **392**, 582 (1998).
[9] L. R. Marim, M. R. Lemes, and A. D. J. Pino, Phys. Rev. A **67**, 033203 (2003).
[10] M. R. Lemes, L. R. Marim, and A. D. J. Pino, Phys. Rev. A **66**, 023203 (2002).
[11] C. Xiao, F. Hagelberg, and W. A. Lester, Phys. Rev. B **66**, 075425 (2002).
[12] I. Rata *et al.*, Phys. Rev. Lett. **85**, 546 (2000).
[13] K. Jackson, M. Pederson, C.-Z. Wang, and K.-M. Ho, Phys. Rev. A **59**, 3685 (1999).
[14] K. M. Ho *et al.*, Nature (London) **392**, 582 (1998).
[15] A. Sieck *et al.*, Phys. Rev. A **56**, 4890 (1997).
[16] K. A. Jackson *et al.*, Phys. Rev. Lett. **93**, 013401 (2004).
[17] A. A. Shavrstburg *et al.*, Chem. Soc. Rev. **30**, 26 (2001).
[18] A. A. Shavrstburg *et al.*, J. Chem. Phys. **112**, 4517 (2000).
[19] S. Yoo *et al.*, J. Am. Chem. Soc. **126**, 13845 (2004).
[20] M. F. Jarrold and V. A. Constant, Phys. Rev. Lett. **67**, 2994 (1991).
[21] M. F. Jarrold and J. E. Bower, J. Phys. Chem. **96**, 9180 (1992).
[22] S. Yoo and X. C. Zeng, Angew. Chem., Int. Ed.. **44**, 1491 (2005).
[23] D. Wales and H. A. Scheraga, Science **285**, 1368 (1999).
[24] V. E. Bazterra *et al.*, Phys. Rev. A **69**, 053202 (2004).
[25] J. A. Becker, Angew. Chem., Int. Ed. **109**, 1390 (1997).
[26] K. A. Jackson, M. Yang, I. Chaudhuri, and Th. Frauenheim, Phys. Rev. A **71**, 033205 (2005).
[27] I. Vasiliev, S. Ougüut, and J. Chelikowsky, Phys. Rev. Lett. **78**, 4805 (1997).
[28] K. Deng, J. Yang, and T. Chan, Phys. Rev. A **61**, 025201 (2000).
[29] J. A. Becker *et al.*, Mater. Sci. Eng., A **217/218**, 1 (1996).
[30] C. Pouchan, D. Begué, and D. Zhang, J. Chem. Phys. **121**, 4628 (2004).
[31] G. Maroulis, D. Begué, and C. Pouchan, J. Chem. Phys. **119**, 794 (2003).
[32] D. Zhang, D. Begué, and C. Pouchan, Chem. Phys. Lett. **398**, 283 (2004).
[33] J. Wang *et al.*, Chem. Phys. Lett. **367**, 448 (2003).
[34] B. Liu *et al.*, J. Chem. Phys. **109**, 9401 (1998).
[35] C. Miller, Science **252**, 1092 (1991).
[36] J. C. Grossman and L. Mitas, Phys. Rev. B **52**, 16735 (1995).
[37] O. Oña *et al.*, Phys. Rev. A **69**, 053202 (2005).
[38] R. L. Johnston and C. Roberts (Springer-Verlag, Heidelberg, 2003).
[39] G. Syswerda, *Third International Conference on Genetic Algorithms* (Morgan Kaufmann, San Mateo, CA, 1989).
[40] D. Whitley, in *Third International Conference on Genetic Algorithms*, edited by J. Schaeffer, (Morgan Kaufmann, San Mateo, CA, 1989).
[41] D. Whitley, *Rocky Mountain Conference on Artificial Intelligence* (Boulder, Denver, CO, 1988).
[42] V. E. Bazterra, M. B. Ferraro, and J. C. Facelli, J. Chem. Phys. **116**, 5984 (2002).
[43] V. E. Bazterra *et al.*, J. Parallel Distrib. Comput. **65**, 48 (2005).
[44] P. J. Hay and W. R. Wadt, J. Chem. Phys. **82**, 270 (1985).
[45] G. Igel-Mann, H. Stoll, and H. Preuss, Mol. Phys. **65**, 1321 (1988).
[46] M. J. Frisch *et al.*, in GAUSSIAN INC. (Pittsburgh PA, 2003).
[47] See EPAPS Document No. E-PLRAAN-73-052603 for the optimized structures at the B3LYP/LANLZDZ level and for the table of maximum dimensions of the Si_n clusters in the directions of their principal axes, at the B3LYP-LanL2DZ level of theory not found with SDDALL. This document can be reached via a direct link in the online article's HTML reference section or via the EPAPS homepage (http://www.aip.org/pubservs/epaps.html).
[48] I. Rata *et al.*, Phys. Rev. Lett. **85**, 546 (2000).
[49] Q. Sun *et al.*, Phys. Rev. Lett. **90**, 135503 (2003).
[50] T. Bachels and R. Schäfer, Chem. Phys. Lett. **324**, 365 (2000).
[51] J. Wang, X. Zhou, G. Wang, and J. Zhao, Phys. Rev. B **71**, 113412 (2005).
[52] M. F. Jarrold and E. C. Honea, J. Phys.: Condens. Matter **95**, 9181 (1991).
[53] Y.-M. Juan, E. Kaxiras, and R. G. Gordon, Phys. Rev. B **51**, 9521 (1995).
[54] K. Jackson *et al.*, Phys. Rev. B **55**, 2549 (1997).
[55] D. Lide, *Handbook of Chemistry and Physics* (CRC Press, Boca Raton, FL, 1993).
[56] P. Fuentealba, Chem. Phys. Lett. **397**, 459 (2004).